ISBN: 978-3-95450-227-1 ISSN: 2673-5490 doi:10.18429/JACoW-IPAC2022-WEPOMS003

BEAM DYNAMICS WITH A SUPERCONDUCTING HARMONIC CAVITY FOR THE SOLEIL UPGRADE

A. Gamelin*, W. Foosang, P. Marchand, R. Nagaoka, Synchrotron SOLEIL, Gif-sur-Yvette, France
N. Yamamoto, KEK, Ibaraki, Japan

Abstract

In 4th generation low emittance synchrotron light sources, harmonic cavities are critical components needed to reach the required performance. However, RF systems with harmonic cavities can be limited by their own set of instabilities. An instability dominated by the coupled-bunch mode $l = 1$ can prevent the RF system from reaching the flat potential condition, hence limiting the maximum bunch lengthening. Here we report how this instability impacts the performance of 3rd and 4th harmonic superconducting cavities for the SOLEIL Upgrade.

INTRODUCTION

The SOLEIL Upgrade project aims to replace the existing storage ring by a 4th generation light source [1–4]. In the framework of the project technical design report (TDR) phase, self-consistent longitudinal beam dynamics simulations are performed to compare different harmonic cavity (HC) technological options. So far, the proposed double RF system comprises:

- A fundamental RF system at 352 MHz, which will provide the required RF voltage and power to compensate for the energy lost by the electron beam and achieve a large enough longitudinal acceptance. It consists of four normal conducting (NC) cavities of the ESRF-EBS type [5, 6], each powered with a 200 kW solid state amplifier (SSA).

- A harmonic RF system, aimed at lengthening the electron bunches in order to preserve low emittance and ensure suitable lifetime. It consists of a cryomodule of the Super-3HC type, similar to that used in SLS and ELETTRA [7–13], which contains two superconducting (SC) passive cavities, tuned to the 3rd or 4th harmonic of SOLEIL (1.06 or 1.41 GHz).

This paper describes the beam dynamics with such a system and compares the respective performance in terms of bunch lengthening of the 3rd and 4th harmonic options for the main operation mode at 500 mA. The TDR lattice and its parameters are presented in [2]; the RF cavity parameters are listed in Table 1. This paper starts with the SC passive HC theory near the flat potential condition, then tracking simulation results are presented showing stable regime, instability regime and the impact of empty buckets in the bunch train.

* alexis.gamelin@synchrotron-soleil.fr

Table 1: Parameters for the RF Cavities

Parameters	MC	HC
Harmonic number m	1	3 or 4
Shunt impedance R (per cavity)	5 MΩ	4.5 GΩ
Unloaded quality factor Q	35 700	10^8
R/Q (per cavity)	140 Ω	45 Ω
Loaded quality factor	6 000	10^8
Cavity number	4	2

SC PASSIVE HC

Let us assume a RF system composed of two "ideal" cavities: a main cavity (MC) with a voltage V_1, a phase ϕ_1, an angular frequency ω_1 and a harmonic cavity (HC) of the m^{th} harmonic with a voltage V_2 and phase ϕ_2. The overall voltage V_{tot} provided by this system at time t is given by:

$$V_{tot}(t) = V_1 \cos(\omega_1 t + \phi_1) + V_2 \cos(m\omega_1 t + \phi_2) . \quad (1)$$

The condition to ensure energy balance for the synchronous particle is:

$$V_{tot}(0) = \frac{U_{loss}}{e} , \quad (2)$$

where U_{loss} corresponds to the energy loss per turn and e is the elementary charge. In such a system, one can adjust the bunch length by controlling the slope of the overall voltage at the synchronous phase, $\alpha_1 = \dot{V}_{tot}(0)$, and its derivative, $\alpha_2 = \ddot{V}_{tot}(0)$. Introducing ξ, as defined in [14]:

$$\xi = \frac{-mV_2 \sin(\phi_2)}{V_1 \sin(\phi_1)} . \quad (3)$$

The system is described by the following equations:

$$\cos(\phi_1) = \frac{U_{loss}}{eV_1} + \xi \frac{\sin(\phi_1)}{m \tan(\phi_2)} , \quad (4)$$

$$V_2 = -\xi \frac{V_1 \sin(\phi_1)}{m \sin(\phi_2)} , \quad (5)$$

$$\tan(\phi_2) = \xi m \tan(\phi_1) . \quad (6)$$

Expressing α_1 and α_2 as a function of ξ:

$$\alpha_1 = \xi\omega_1 \sin(\phi_1) \left(1 - \frac{1}{\xi}\right) , \quad (7)$$

$$\alpha_2 = -V_1{\omega_1}^2 \left[\cos(\phi_1) - \xi m \frac{\sin(\phi_1)}{\tan(\phi_2)}\right] . \quad (8)$$

One can see that the value $\xi = 1$ cancels both α_1 and α_2 and that going from $\xi \leq 1$ to $\xi \geq 1$ implies a change of sign

ISBN: 978-3-95450-227-1 ISSN: 2673-5490 doi:10.18429/JACoW-IPAC2022-WEPOMS003

of the RF voltage slope. The case $\xi = 1$ in Eq. (4) to (6), which corresponds to $\alpha_1 = \alpha_2 = 0$ is called Flat Potential (FP) condition.

If the HC is passive, for a fixed V_1, its tuning angle ψ is the only free parameter, which allows to adjust its beam induced voltage. Neglecting bunch form factors, V_2 can be expressed as:

$$V_2 = 2I_0 R\cos\psi \approx I_0 \frac{R}{Q}\frac{m\omega_1}{\Delta\omega}\sin\psi\,, \tag{9}$$

where I_0 is the beam current and $\Delta\omega$ is the HC detuning. The FP condition can only be met for a single value of the RI_0 product:

$$RI_0 = \frac{V_1\cos\phi_1}{2m^2\cos\psi^2}\,. \tag{10}$$

More generally, α_2 is non-zero and for $\xi = 1$ it is fixed to:

$$\alpha_2 = -{V_1\omega_1}^2\left[\frac{U_{loss}}{eV_1} - \frac{m^2-1}{m}\frac{\sin(\phi_1)}{\tan(\psi)}\right]. \tag{11}$$

To distinguish this case ($\xi = 1$ in Eq. 4 and 5 corresponding to $\alpha_1 = 0$ and $\alpha_2 \neq 0$) from the FP case, it is called the "Near Flat Potential" (NFP) condition. The main consequence of a non zero α_2 is an asymmetry in the bunch profiles.

In the particular case of a SC passive HC, as the dissipation is negligible, the tuning angle is fixed to $\psi \approx \pi/2$ within the useful tuning range. In that case, the previous set of equations is simplified to:

$$\cos(\phi_1) \approx \frac{U_{loss}}{eV_1}\,, \tag{12}$$

$$V_2 \approx \xi\frac{V_1\sin(\phi_1)}{m} \approx I_0\frac{R}{Q}\frac{m\omega_1}{\Delta\omega}\,, \tag{13}$$

$$\alpha_2 \approx -\frac{{\omega_1}^2 U_{loss}}{e}\,. \tag{14}$$

So for a SC passive HC, in first approximation, the MC phase is the same as the one used without HC and the second derivative of the RF voltage α_2 can never be cancelled.

SIMULATION RESULTS

In this section, beam dynamics tracking simulation results are presented. The simulations are done using mbtrack2 [15], which models cavity physics in a fully self consistent way with a very similar implementation to that of mbtrack [16].

Stable Regime

Figure 1 shows the stable settings found by tracking for the 3rd and 4th HC. Each point on that plot corresponds to a HC tuning for which the beam is stable and its corresponding bunch length and ξ values have been computed. The maximum bunch length that can be obtained is about 50 ps for the 3rd HC and 34 ps for the 4th HC, to be compared to the natural bunch length of 9 ps without HC. These limits are reached at different ξ values, $\xi = 1.01$ and $\xi = 0.97$ for 3rd and 4th harmonic, beyond which the beam starts to be unstable.

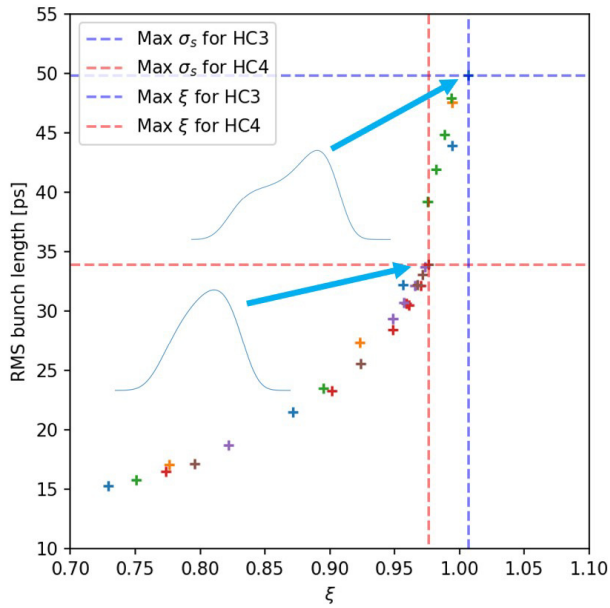

Figure 1: RMS bunch length versus ξ from different tracking simulations for the 3rd and 4th HC. The bunch profile associated to the maximum RMS bunch length is shown for both harmonics.

Another expected effect of HCs is a reduction of the incoherent synchrotron frequency f_s from its natural value without HCs f_{s0}. This reduction, in the small oscillation approximation, can be estimated as:

$${f_s}^2 \approx f_{s0}^2\left[1-\xi\right]\,. \tag{15}$$

This equation agrees rather well with the tracking results for $\xi \leq 0.9$. Closer to the NFP, f_s computed from tracking does not decrease to zero but tends to 200 Hz for the 3rd harmonic and to 360 Hz for the 4th one. As the 3rd HC allows to operate closer to the NFP, its 110 Hz synchrotron frequency spread is larger than the 55 Hz one obtained from the 4th harmonic. Significant Landau damping can be expected from such a spread in f_s.

Instability

The instability limiting further bunch lengthening is of the same nature for both harmonics. It is dominated by the coupled bunch mode $l = 1$ as shown by the beam coherent spectrum in Fig. 2.

This instability exhibits the same specificities as the ones reported in [17] under the name "coupled bunch mode $l = 1$ instability" using perturbation-theory or in [18] using tracking and named "periodic transient beam loading" instability. It seems to happen when the usual stable solution, found in the case of a uniform beam filling where all the bunches have the same profile, breaks down. Beyond the threshold, the bunches have different profiles. The system falls back to a quasi-stable state slowly drifting through the bunch index space with rather long time period ($f \approx$ Hz), which depends on the cavity parameters. The behaviour this instability is thus quite different from usual coupled bunch instabilities.

ISBN: 978-3-95450-227-1 ISSN: 2673-5490 doi:10.18429/JACoW-IPAC2022-WEPOMS003

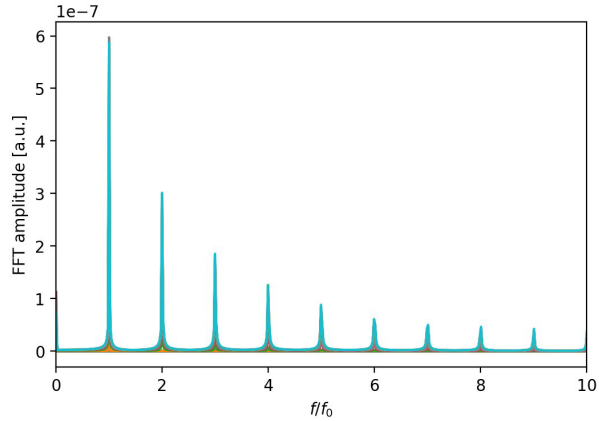

Figure 2: Beam coherent spectrum during the instability.

This situation is described in Fig. 3, where the quasi-stable state is shown at a given turn. It shows variations of the RMS bunch length and ξ along the bunch index during this instability. Despite the initial uniform filling pattern, each bunch has a different profile: the highest ξ values, around 1.06, correspond to double bump bunch and other bunches with lower ξ values have single bump shapes.

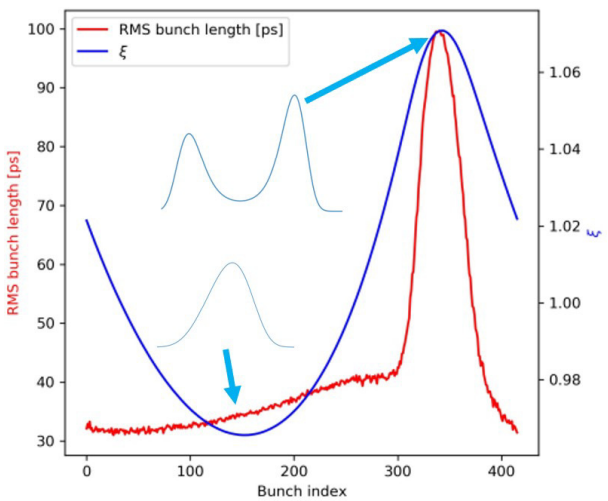

Figure 3: Variation of the RMS bunch length and ξ along the bunch index during the instability.

In [18], it is found that the instability threshold increases with bunch length. As the 3rd HC naturally produces longer bunches compared to the 4th one for the same ξ value, it explains why the threshold is reduced for the 4th HC.

This type of instability has been observed in many simulations for the SOLEIL Upgrade case, for passive SC HC but also for active or passive NC HC. It has also been observed in simulations for other machines (Diamond-II, HALF, ...) and experimentally at MAX IV [19].

Gaps in the Filling Pattern

The instability dominated by the coupled bunch mode $l = 1$ seems to be strongly suppressed when the filling pattern is no longer uniform. When gaps of empty buckets are introduced in the bunch train to reduce ion trapping, or when there are strong bunch to bunch current variations induced by injection imperfections, the transient beam loading leads to a reduction of the average bunch lengthening compared to the uniform filling case. In that case, operating close to the NFP is no longer efficient as it leads to very strong bunch phase and length variations along the filling pattern.

In all the simulated cases, the different bunch distributions were stable, i.e. not showing periodic variation as it is the case for this instability, at least in the limited timescale for which they were simulated. The values corresponding to the highest Touschek lifetime in the stable tuning range (for a typical bunch of the train) are reported in Table 2.

Table 2: Touschek Lifetime Increase Factor T with Various Gap Length

m	Gap length	T	Mean RMS	Mean FWHM
3	no gap	5.7	50 ps	98 ps
3	1 bunch	4.7	40 ps	94 ps
3	2 bunch	4.3	36 ps	85 ps
3	5 bunch	3.5	29 ps	70 ps
3	10 bunch	2.9	24 ps	58 ps
4	no gap	4.2	34 ps	91 ps
4	1 bunch	3.4	28 ps	71 ps
4	2 bunch	3.2	27 ps	66 ps
4	5 bunch	2.7	22 ps	54 ps
4	10 bunch	2.2	18 ps	44 ps

The Touschek lifetime gain factor T is defined as [20]:

$$T = \frac{\tau}{\tau_0} \approx \frac{\int \rho_0{}^2(z)dz}{\int \rho^2(z)dz} \tag{16}$$

where τ and ρ are respectively the mean lifetime and longitudinal charge density with HC. The subscript 0 on the same symbols corresponds to quantities without HC bunch lengthening.

CONCLUSION

Tracking simulations show that, using a SC passive HC, one can achieve relatively large Touschek lifetime increase factors for the SOLEIL Upgrade main operation mode (500 mA in uniform filling): up to 5.7 with 3rd HC and 4.2 with 4th HC, limited by an instability dominated by the coupled bunch mode $l = 1$ in both cases. Non-uniformities of the filling pattern suppress this instability but reduce the possible bunch lengthening. Other operation modes and alternative solutions (active and passive NC HC) are also being investigated.

ACKNOWLEDGEMENTS

The authors thank P. Tavares, F. Cullinan and T. Olsson for fruitful discussions and advice. This work has been accomplished as part of a RF collaboration between different labs (KEK, PSI, ESRF, BESSY and SOLEIL), we thank our partners for the useful exchanges.

ISBN: 978-3-95450-227-1 ISSN: 2673-5490 doi:10.18429/JACoW-IPAC2022-WEPOMS003

REFERENCES

[1] "Conceptual Design Report - Synchrotron SOLEIL Upgrade," 2021.

[2] A. Loulergue *et al.*, "TDR Baseline Lattice for the SOLEIL Upgrade," presented at IPAC'22, Bangkok, Thailand, Jun. 2022, paper TUPOMS004, this conference.

[3] A. Nadji, "Synchrotron SOLEIL Upgrade Project," in *Proc. IPAC'21*, Campinas, Brazil, May 2021, pp. 463–465. doi: 10.18429/JACoW-IPAC2021-MOPAB131.

[4] A. Loulergue *et al.*, "CDR Baseline for the Upgrade of SOLEIL," in *Proc. IPAC'21*, Campinas, Brazil, May 2021, pp. 1485–1488. doi: 10.18429/JACoW-IPAC2021-TUPAB054

[5] J. Jacob, P. B. Borowiec, A. D'Elia, G. Gautier, and V. Serrière, "ESRF-EBS 352.37 MHz Radio Frequency System," in *Proc. IPAC'21*, Campinas, Brazil, May 2021, pp. 395–398. doi: 10.18429/JACoW-IPAC2021-MOPAB108

[6] A. D'Elia, J. Jacob, and V. Serrière, "ESRF-EBS 352 MHz HOM Damped RF Cavities," in *Proc. IPAC'21*, Campinas, Brazil, May 2021, pp. 1034–1036. doi: 10.18429/JACoW-IPAC2021-MOPAB333

[7] P. Marchand, "Possible Upgrading of the SLS RF System for Improving the Beam Lifetime," in *Proc. PAC'99*, New York, NY, USA, Mar. 1999, paper MOP138, pp. 889–891.

[8] M. Svandrlik *et al.*, "The SUPER-3HC Project: an Idle Superconducting Harmonic Cavity for Bunch Length Manipulation," in *Proc. EPAC'00*, Vienna, Austria, Jun. 2000, paper THB7B10, pp. 2052–2054.

[9] S. Chel *et al.*, "Super-3HC Cryomodule: Layout and First Tests," in *Proc. EPAC'02*, Paris, France, Jun. 2002, paper THPDO010, pp. 2217-2219.

[10] M. Pedrozzi *et al.*, "SLS Operational Performance with Third Harmonic Superconducting System," in *Proc. SRF'03*, Lübeck, Germany, Sep. 2003, paper MOP25, pp. 91–94.

[11] G. Penco, P. Craievich, A. Fabris, C. Pasotti, and M. Svandrlik, "First Year of Operation of SUPER-3HC at ELETTRA," in *Proc. EPAC'04*, Lucerne, Switzerland, Jul. 2004, paper TUPKF021, pp. 1009-1011.

[12] P. Marchand, "Superconducting RF cavities for synchrotron light sources," in *Proc. EPAC'04*, Lucerne, Switzerland, Jul. 2004, paper MOYCH03, pp. 21–25.

[13] G. Penco and M. Svandrlik, "Experimental studies on transient beam loading effects in the presence of a superconducting third harmonic cavity," *Phys. Rev. Spec. Top. Accel Beams*, vol. 9, no. 4, p. 044 401, Apr. 10, 2006. doi: 10.1103/PhysRevSTAB.9.044401

[14] R. A. Bosch, K. J. Kleman, and J. J. Bisognano, "Robinson instabilities with a higher-harmonic cavity," *Phys. Rev. Spec. Top. Accel Beams*, vol. 4, no. 7, p. 074 401, 2001. doi: 10.1103/PhysRevSTAB.4.074401

[15] A. Gamelin, W. Foosang, and R. Nagaoka, "mbtrack2, a Collective Effect Library in Python," in *Proc. IPAC'21*, Campinas, Brazil, May 2021, pp. 282–285. doi: 10.18429/JACoW-IPAC2021-MOPAB070

[16] N. Yamamoto, A. Gamelin, and R. Nagaoka, "Investigation of Longitudinal Beam Dynamics With Harmonic Cavities by Using the Code Mbtrack," in *Proc. IPAC'19*, Melbourne, Australia, May 2019, pp. 178–180. doi:10.18429/JACoW-IPAC2019-MOPGW039

[17] M. Venturini, "Passive higher-harmonic rf cavities with general settings and multibunch instabilities in electron storage rings," *Phys. Rev. Accel. Beams*, vol. 21, no. 11, p. 114 404, 2018. doi: 10.1103/PhysRevAccelBeams.21.114404

[18] T. He, W. Li, Z. Bai, and L. Wang, "Periodic transient beam loading effect with passive harmonic cavities in electron storage rings," *Phys. Rev. Accel. Beams*, vol. 25, no. 2, p. 024 401, Feb. 3, 2022, Publisher: American Physical Society. doi: 10.1103/PhysRevAccelBeams.25.024401

[19] F. Cullinan, A. Andersson, J. Breunlin, M. Brosi, and P. F. Tavares, "Longitudinal beam dynamics in ultra-low emittance rings," Karlsruhe, Germany, Presented at I.FAST Workshop on beam diagnostics and beam dynamics in ultra-low emittance rings, 2022.

[20] R. Warnock and M. Venturini, "Equilibrium of an arbitrary bunch train in presence of a passive harmonic cavity: Solution through coupled haïssinski equations," *Phys. Rev. Accel. Beams*, vol. 23, no. 6, p. 064 403, Jun. 24, 2020. doi: 10.1103/PhysRevAccelBeams.23.064403